Available online at www.sciencedirect.com
ScienceDirect
Biochimica et Biophysica Acta 1777 (2008) 48–54
Biochimica et Biophysica Acta BBA
www.elsevier.com/locate/bbabio

# Modified glutamine catabolism in macrophages of *Ucp2* knock-out mice

Tobias Nübel [a], Yalin Emre [a], Daniel Rabier [b], Bernadette Chadefaux [b], Daniel Ricquier [a,b], Frédéric Bouillaud [a,*]

[a] *BIOTRAM, Université Paris Descartes, CNRS UPR9078, Faculté de Médecine Necker-Enfants Malades, 156 rue de Vaugirard 75730 Paris, France*
[b] *Laboratoire de Biochimie métabolique, Hopital Necker-Enfants Malades, 149, rue de Sèvres, 75743 Paris Cedex 15, France*

Received 27 June 2007; received in revised form 17 October 2007; accepted 5 November 2007
Available online 12 November 2007

**Abstract**

Uncoupling protein 2 (UCP2) belongs to a family of transporters of the mitochondrial inner membrane and is reported to uncouple respiration from ATP synthesis. Our observation that the amino acid glutamine specifically induces UCP2 protein expression prompted us to investigate metabolic consequences of a UCP2 knockdown (*Ucp2-KO*) when glutamine is offered as a substrate. We found that *Ucp2-KO* macrophages incubated in the presence of glutamine exhibit a lower ammonium release, a decreased respiratory rate, and an intracellular accumulation of aspartate. Therefore, we conclude that UCP2 expression is required for efficient oxidation of glutamine in macrophages. This role of UCP2 in glutamine metabolism appears independent from the uncoupling activity of UCP2.


*Keywords:* UCP2; Macrophage; Uncoupling protein; Mitochondria; Glutamine; Glutaminolysis

## 1. Introduction

Uncoupling protein 2 (UCP2) is located in the inner membrane of the mitochondria. UCP2 was found to be expressed in diverse tissues in mammals, as e.g. in pancreatic islets and in many cells of the immune system including macrophages [1–3]. UCP2 belongs to the family of mitochondrial anion carriers and shows high similarity to UCP1, the brown adipose tissue uncoupling protein [4,5]. Mild uncoupling of mitochondria (reviewed in [6]) was proposed as a means to prevent superoxide production by the respiratory complexes I and III [7]. Consequently, such a role has been proposed for UCP2 [8]. However, its exact role remains discussed [2,9]. UCP2 was shown to play a regulatory role in macrophage mediated immunity and/or inflammatory responsiveness of these cells [3,5,10–12]. It was also characterized as a negative regulator of insulin secretion in pancreatic beta-cells [13]. Recently the causes of the enhanced macrophage activity in *Ucp2-KO* mice have been studied in further details [14].

Immune cells utilize glutamine besides glucose at very high levels and the rate of glutamine utilization by these cells is either similar to or even greater than that of glucose [15,16]. Incomplete oxidation of glucose or glutamine (glutaminolysis) takes place in immune cells. Glucose is converted almost totally into lactate and glutamine into ammonium, glutamate, aspartate and lactate. Fig. 1 provides a schematic overview over the steps of glutamine catabolism relevant here.

The UCP2mRNA contains a long 5′ untranslated region in which a short upstream open reading frame (uORF) is present. According to our work, this results in a constitutive inhibition of translation of UCP2 mRNA [17,18]. More recently, we have shown that the presence of glutamine in the surrounding medium relieves the constitutive inhibition of UCP2 translation by the uORF [19]. Accordingly, we proposed that UCP2 may be involved in the oxidative metabolism of glutamine [20]. Primary cultures of bone marrow derived macrophages (BMDM) allowed us to compare cells from "wild type" mice (*Ucp2-WT*) with cells obtained from mice where the Ucp2 gene has been invalidated by homologous recombination (*Ucp2-KO*) [14,21].

*Abbreviations:* UCP, uncoupling protein; EBSS, Earle's balanced saline solution; BMDM, bone marrow derived macrophages; FCS, foetal bovine serum; MCSF, macrophage colony-stimulating factor; AOA, aminooxyacetic acid; DON, 6-diazo 5-oxo norleucine

* Corresponding author. Fax: +33 1 40 61 56 73.
*E-mail address:* bouillaud@necker.fr (F. Bouillaud).

0005-2728/$ - see front matter © 2007 Elsevier B.V. All rights reserved.
doi:10.1016/j.bbabio.2007.11.002

## 2. Materials and methods

### 2.1. Reagents

PBS, RPMI 1640 with glutamax, Earle's balanced saline solution (EBSS, containing 5 mM glucose) and glutamine were purchased from Life Technologies SARL, Cergy Pontoise, France, and foetal calf serum (FCS) from PAA Laboratories GmbH, Pasching, Austria. Anti-porin antibody was from Molecular Probes Europe BV, Leiden, The Netherlands. Anti-hUCP2-605 and rabbit anti-IgG were generated in our laboratory and used as previously described [17]. ECL-kit was obtained from Amersham Biosciences, Buckinghamshire, UK and ENLITEN®Luciferase/Luciferin (rLuc/Luc) Reagent from Promega Corporation, Madison, USA. Other chemicals, mouse anti-IgG, myokinase and DNase were obtained from Sigma-Aldrich St Quentin-Fallavier France.

### 2.2. Cell culture conditions

BMDM were isolated from *Ucp2-KO* mice in which the Ucp2 gene had been invalidated by homologous recombination [10] and from their littermate control (*Ucp2-WT*) as previously described [14]. The experiments were made by incubating BMDM in EBSS medium in the presence or absence of glutamine (2 mM): RPMI media were exchanged against EBSS containing glutamine or not and cells were further cultivated up to 16 h (overnight). Incubations in the absence of glucose were made in PBS to which was added 1.3 mM $Ca^{2+}$ and 50 μM $Mg^{2+}$, this medium is referred to as "PBS" hereafter. It was checked by the use of the WST assay (Roche Diagnostics, Mannheim, Germany) measuring metabolic activity of mitochondria or by measuring the percentage of cells in sub-G1 phase, that BMDM could withstand such treatments.

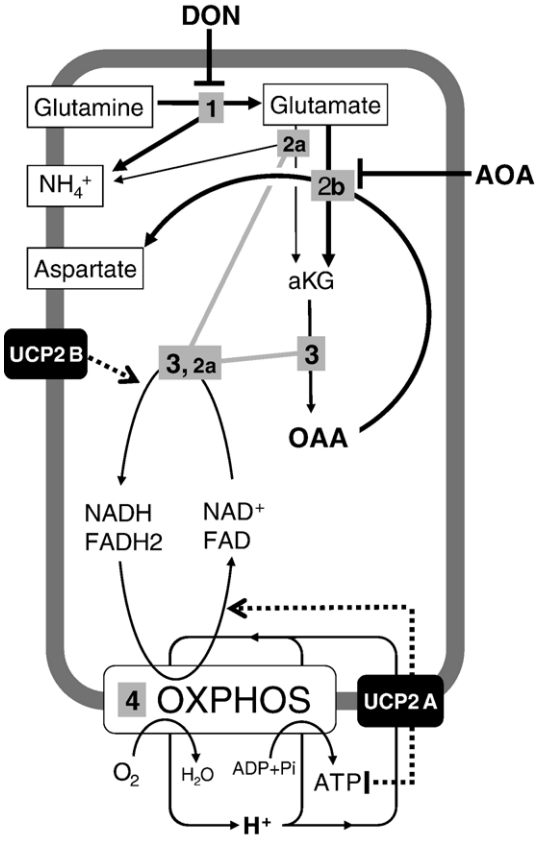


Fig. 1. Intramitochondrial metabolism of glutamine. The mitochondrial inner membrane is schematized as a thick gray line. aKG: alpha-keto-glutarate, OAA oxaloacetic acid. Steps of the metabolism of glutamine relevant here are numbered. 1: Loss of first ammonium group (glutaminase) inhibited by DON; 2: loss of the second ammonium group (2a: glutamate dehydrogenase, 2b: transaminase inhibited by AOA); 3: oxidative metabolism in the Krebs cycle. 4: "OXPHOS" with respiratory chain coupling reoxidation of coenzymes to creation of a proton gradient and the phosphorylating unit (FoF1ATPase, Phosphate and ATP/ADP transporters) using this proton gradient to generate ATP by phosphorylation of ADP. UCP2 is placed in two different positions: "A" UCP2 acts as a proton leak (uncoupling effect) that dissipates the electrochemical gradient, favorises reoxidation of coenzymes and decreases ATP/ADP ratio. In position "B" UCP2 increases the availability of reduced coenzymes to the respiratory chain. This study supports the "UCP2 B" hypothesis.

### 2.3. Western blot analysis

Whole cellular extract from macrophages were prepared as follows: after washing in PBS the pellet of cells was resuspended in solubilisation buffer (50 mM Tris pH 7.8, 150 mM NaCl, 1% NP-40) with protease inhibitors (1 μg/ml pepstatin, 4 μg/ml aprotinin, 2 μg/ml leupeptin, 5 μg/ml bestatin), after 30 min in ice this was centrifuged at 10 000 ×g for 20 min and the supernatant was used. To prepare mitochondrial extracts, harvested macrophages were resuspended in an isolation buffer (250 mM sucrose, 10 mM Tris-Base, 2 μg/ml DNase, pH 7.4) with protease inhibitors. After three freeze-and-thaw cycles in liquid nitrogen and incubation in 37 °C, respectively, unbroken cells and nuclei were removed by centrifugation (750 ×g, 10 min). The supernatant was centrifuged for 20 min at 12 000 ×g and pelleted mitochondria were resuspended in an isolation buffer with protease inhibitors. Protein content was determined by use of Sigma Procedure TPRO-562 according to the manufacturer's protocol. Mitochondrial protein extracts were loaded onto polyacrylamide gels, separated by electrophoresis and transferred onto nitrocellulose membrane as previously described [17]. Western blots were hybridized with appropriate antibodies under the following conditions: UCP2, hUCP2-605 antibody (at 1/2000 dilution) and rabbit anti-IgG (at 1/3000 dilution); porin, anti-porin antibody (Molecular Probes, at 1/4000 dilution) and mouse anti-IgG (Sigma-Aldrich, at 1/3000 dilution). Direct recording of the chemiluminescence (ECL-kit) was performed using the GeneGnome analyzer (Ozyme, St-Quentin Yvelines, France).

### 2.4. Quantitative ammonia and amino acid analysis

Macrophages were harvested and homogenized by sonication with a Branson Digital Sonifier W-450D (Branson, Danbury, USA). Homogenized samples were deproteinized by adding 1/10 volume of sulfosalicylic acid solution (400 g/l) and centrifuged (10 000 ×g, 5 min). Afterwards, 40 μl of the supernatant was used for quantitative amino acid analysis by ion-exchange chromatography and injected into a JEOL Aminotac JLC 500/V amino acid analyzer (JEOL EUROPE SA, Croissy-sur-Seine, France) calibrated by analyzing calibration standard of known concentration. Retention time was used for amino acid identification and integration was used for quantification.

### 2.5. Measurements linked to mitochondrial activity

Oxygen consumption was measured in an oxygraph chamber (Hansatech Instruments Ltd., Norfolk, England). Oligomycin (0.5 μg/ml final) was used to evaluate the coupling of respiration in intact cells.

ATP was analyzed luminometrically (Lumat LB 9501, Berthold Technologies France SA, Thoiry, France) using a 10 s signal integration time. Lysis of approximately 4 million cells was performed with 0.5 ml Passive Lysis Buffer, 5× (Promega corporation, Madison, USA). 10 μl of this lysate was diluted in 40 μl H2O and 50 μl of rLuc/Luc-Reagent (Promega Corporation, Madison, USA). For quantification of ADP 200 μl of the cell lysate was added to 800 μl of 50 mM Tris/HCl, 0.5 mM EGTA, pH 8 and incubated for 30 min with 1 U/ml myokinase at room temperature, then ATP concentration was determined as above. ADP concentrations were obtained by subtraction of determined ATP concentrations: [ADP]=[ATP] (after myokinase)−[ATP] (without myokinase).

Mitochondrial NADH/NAD+ ratios were estimated indirectly via quantitative analysis of β-hydroxybutyrate and acetoacetate. Ratios of β-hydroxybutyrate to acetoacetate reflect directly the redox-state of the mitochondria and thereby correspond directly with mitochondrial ratios of NADH/NAD+ [22–24]. Quantification of β-hydroxybutyrate and acetoacetate was performed spectrophotometrically using a dual-wavelength spectrophotometer (SLM-Aminco

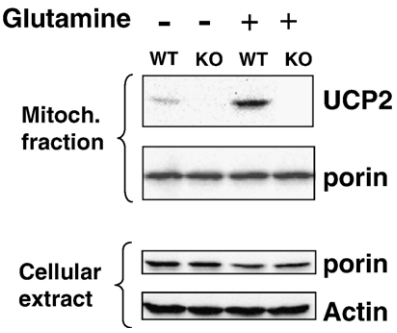


Fig. 2. Induction of UCP2 expression. After overnight incubation of BMDM, isolated from *UCP2-WT* and *UCP2-KO* mice, in EBSS in the presence or absence of 2 mM glutamine. Top: Mitochondrial fractions were prepared and examined for UCP2 protein levels by Western blot analysis. As a control, membranes were re-probed with anti-porin antibody. Bottom: The gel was loaded with extracts from whole cells probed with actin and porin antibodies to examine possible changes in mitochondrial content.

DW-2A; SLM Instruments, Inc., Urbana, IL) and differential analysis. All reactions run at 30 °C in a final volume of 400 µl. After adding buffer and coenzymes to the sample absorbance A1 was measured, the reaction was started by addition of the appropriate enzyme. Measurement of absorbance A2 was recorded after 20 min. The difference (A2 − A1) of the reagent blank was subtracted from the difference (A2 − A1) of the sample. Concentrations were determined by the use of standard of known concentration. Assay conditions for determination of acetoacetate in 200 µl of cell culture media: 0.26 mM NADH and 580 U/l hydroxybutyrate dehydrogenase in 80 mM Tris/HCl-buffer, pH 7. Assay conditions for quantification of β-hydroxybutyrate in 200 µl of cell culture media: 10 mM NAD+ and 580 U/l hydroxybutyrate dehydrogenase in 80 mM Tris/HCl-buffer, pH 9.5.

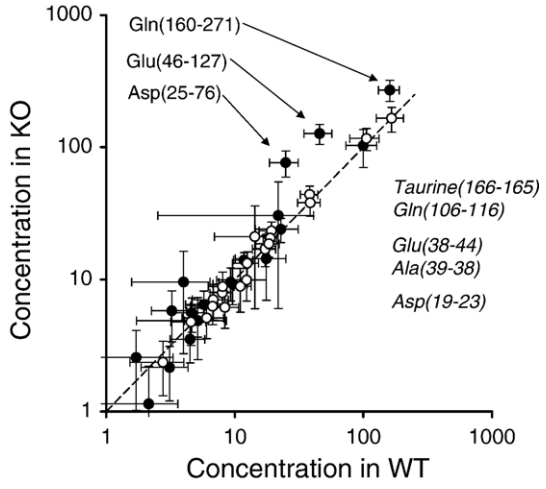


Fig. 3. Internal amino acids content of BMDM. BMDM were incubated overnight (14–16 h) in EBSS in the presence or absence of 2 mM glutamine. After preparation of total cell extracts of about 4 million cells, metabolite quantitation was performed by ion-exchange chromatography (see Materials and methods section). The concentrations of amino acids in these cellular extracts (in µM) are plotted on a biparametric graph: each dot represents a single amino acid, the *X* ordinate of the dot corresponds to its concentration in the *Ucp2-WT* BMDM extract, and the *Y* ordinate to its concentration in the *Ucp2-KO* BMDM extract. The error bars represent the s.e.m. ($N=7$ independent experiments). White dots represent data obtained in the absence of glutamine and black dots in its presence. The actual values (*X* and *Y* ordinate) of concentrations of amino acid of special interest are shown on the graph. Indications italicized refer to measures in the absence of glutamine, and those in plain text to values obtained in the presence of glutamine.

### 2.6. Quantification of glutamine oxidation with [U-14C]glutamine

Macrophages were cultured overnight (16 h) in PBS with or without 2 mM glutamine and afterwards 0.175 µCi [U-14C]glutamine was added for 90 min. The generated 14CO2 by approximately 4 million of macrophages was captured in 70 µl 1 M KOH and disintegration events per minute (dpm) were counted after the addition of 2 ml liquid-scintillations-mix OptiPhase 'HiSafe'3 in a Liquid Scintillation Analyzer Tri-Carb 2100TR (Packard, GMI, Minnesota, USA).

## 3. Results

The presence of glutamine during overnight incubation in EBSS allowed a robust expression of UCP2 whereas the absence of glutamine was associated with much lower expression level (Fig. 2). As expected, no immunoreactive protein could be detected in macrophages originating from *Ucp2-KO* mice. Examination of relative immunoreactivity of porin and actin in whole cell extracts indicated no difference between BMDM originating from *Ucp2-KO* or *-WT* mice, without noticeable effect of glutamine exposure.

The purpose of all the following experiments was to compare *Ucp2-KO* to *Ucp2-WT* BMDM in the same conditions. Therefore, experiments were made with paired overnight incubations of *Ucp2-KO* and *Ucp2-WT* BMDM in the presence or absence of glutamine.

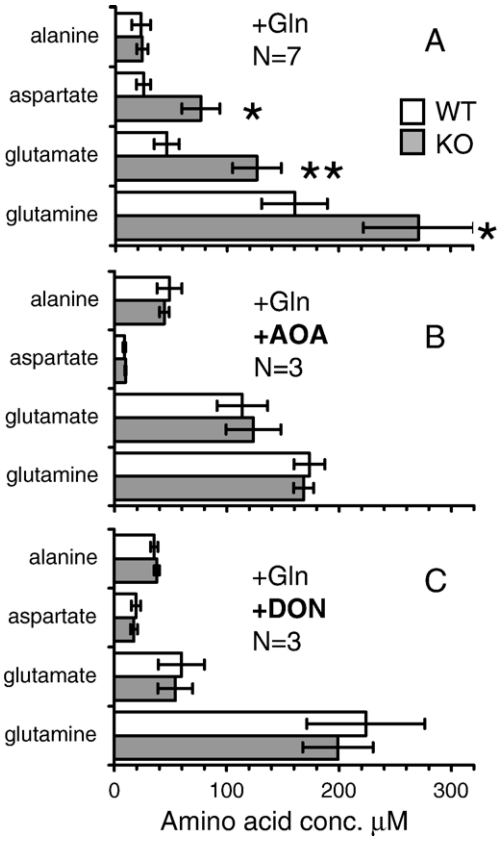


Fig. 4. Effect of inhibitors. Measurement of internal content in the amino acids alanine (taken as an internal control), aspartate, glutamate, and glutamine, in BMDM incubated overnight in EBSS plus 2 mM glutamine. WT: *Ucp2-WT* BMDM, KO: *Ucp2-KO* BMDM, values are shown ± s.e.m. A: In the absence of inhibitors, the values are the same as those shown in Fig. 3, $*P<0.05$, $**P<0.01$ (*t* test). B: In the presence of 5 mM of AOA. C: In the presence of 20 mM of DON.

Comparison of the cellular content in amino acids between *Ucp2-WT* and *Ucp2-KO* BMDM is shown (Fig. 3). When there is no difference between the two types of BMDM dots are aligned according to the first diagonal. This is observed when *Ucp2-WT* and *Ucp2-KO* BMDM are compared in the EBSS medium (Fig. 3, white dots). In contrast, when glutamine was present *Ucp2-KO* BMDM accumulated more glutamine, glutamate and aspartic acid (Fig. 3A, black dots). The logarithmic scale used minimizes the actual differences which can be seen in Fig. 4. Addition of 20 mM of the glutaminase inhibitor DON or of 5 mM of the transaminase inhibitor AOA abolished the differences in intracellular glutamine, glutamate and aspartate concentrations between *Ucp2-WT* and *Ucp2-KO* BMDM (Fig. 4).

The cellular respiration of BMDM was recorded after incubation of BMDM in EBSS or EBSS+Gln as for the previous experiment. After 16 h in EBSS both types of BMDM showed a similar respiratory rate (Fig. 5A top). In contrast, after 16 h in

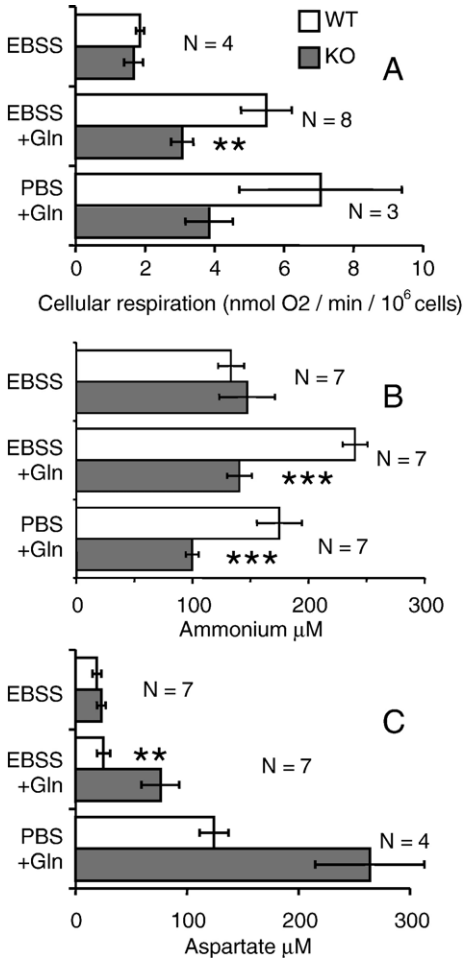


Fig. 5. Oxidative metabolism. A) Respiration was determined in BMDM that had been incubated overnight in EBSS±2 mM glutamine. The number of independent experiment (*N*) is indicated, mean values are shown ±s.e.m. $^{**}P<0.01$, $^{***}P<0.001$ (*t* test). B) The ammonium ion concentration was determined in the same cellular extracts as in Fig. 3. The value obtained with BMDM incubated in PBS+Gln is also shown. C) Aspartate concentration in cellular extracts. The values in EBSS+Gln are shown again for the comparison with the values obtained when BMDM were incubated in PBS+Gln.

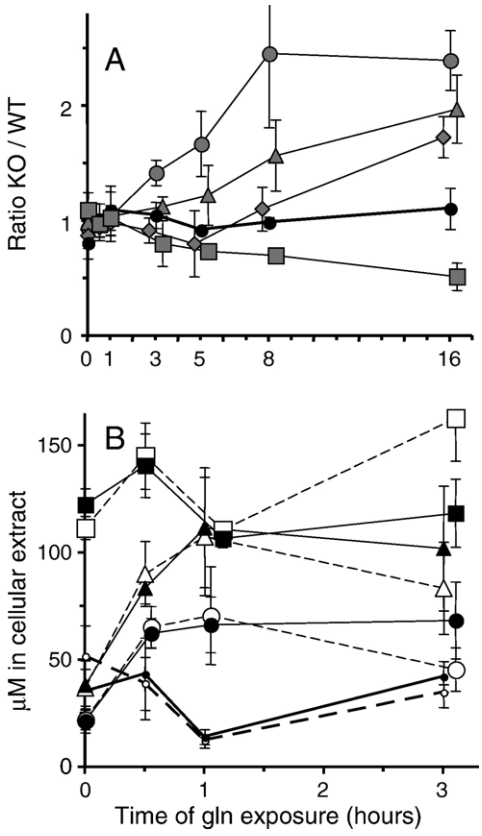


Fig. 6. Kinetic. A) The mean±s.e.m. values of the ratio between concentration of glutamine (diamonds), glutamate (triangles), aspartate (circles), ammonium (squares) and alanine (thick black line and small black circles), are shown before glutamine addition: time zero (*N*=4), 30 min (*N*=3), 1 (*N*=2), 3 (*N*=4), 5 (*N*=2), 8 (*N*=3) and 16 (*N*=4) hours after glutamine addition. B) Actual values of concentration of metabolites in cellular extracts during the 0–3 h period of the experiments shown in A. For clarity the glutamine concentration is not shown. Symbols as above with empty symbols and dotted line for *Ucp2-WT* BMDM, black symbols and solid line for *Ucp2-KO* BMDM.

EBSS+Gln *Ucp2-WT* BMDM showed a doubled respiratory rate when compared to *Ucp2-KO* BMDM (Fig. 5A middle). This appeared to be due to an increase in respiration induced by glutamine in WT rather than to a decrease in the KO. The same difference was observed in experiments where BMDM were incubated in a medium in which glutamine was the only available substrate (Fig. 5A bottom). The respiratory rate of BMDM in the presence of oligomycin, an inhibitor of the mitochondrial Fo-F1 ATP synthase, is explained by ion cycling across the mitochondrial inner membrane. Activation of uncoupling function of a UCP increases the respiratory rate in the presence of oligomycin (see Fig. 6B of [25] for a recent example) and decreases the ratio between the spontaneous respiratory rate and the rate observed after addition of oligomycin. After incubation in EBSS+Glutamine for 16 h this ratio was 5.7±1.4 with *Ucp2-WT* BMDM and 4.4±0.67 with the *Ucp2-KO* BMDM (*N*=5 *P*=0.23). Therefore these ratios provided evidence against a relatively uncoupled state of mitochondria in *Ucp2-WT* BMDM when compared to *Ucp2-KO* BMDM.

Ammonium ion is a final metabolite of glutamine oxidation (Fig. 1). In the absence of glutamine similar concentration of

ammonium was found in both types of BMDM. When glutamine was present ammonium content was doubled in *Ucp2-WT* BMDM compared to *Ucp2-KO* BMDM (Fig. 5B) independently from presence of glucose. While the relative difference in aspartate concentration between *Ucp2-WT* and *Ucp2-KO* BMDM remained the same, the absolute cellular content in aspartate was greatly enhanced in the absence of glucose (Fig. 5C).

Kinetic experiments were performed to examine the order of accumulation of the early metabolites of glutamine catabolism in *Ucp2-KO* BMDM (Fig. 6). To evidence relative accumulation in *Ucp2-KO* BMDM the ratio between metabolite concentration in the two types of BMDM was calculated (Fig. 6A). As expected, the ratio remained around one for alanine. After 3 h accumulation of aspartate in *Ucp2-KO* BMDM (ratio above one) was detected and followed by glutamate and finally by glutamine accumulation. Consistent with above (Fig. 5B) the ratio decreased for the ammonium ion. This representation indicates that during the first hours of incubation the two types of BMDM did not behave differently but provides no information about the appearance of glutamine metabolites. Representation of amino acid concentration during this early phase of glutamine exposure is shown in Fig. 6B. The intracellular content in aspartate and glutamate increased quickly in the same manner for both types of BMDM. Identical kinetics for the cellular content in ammonium ion and alanine was also observed (Fig. 6B). Therefore, these experiments showed that the kinetic accumulation of glutamine metabolites could be divided in two periods: i) an early phase from zero to less than 3 h, with no difference between both types of BMDM. ii) A later phase 3–16 h during which the *Ucp2-WT* produces more ammonium and the *Ucp2-KO* accumulates aspartate. These experiments provided information about the relative activity of glutaminase and transaminase (steps 1 and 2b in Fig. 1) within living BMDM but provided no indication about the glutamate dehydrogenase (step 2a in Fig. 1). The dosage of the activity of this enzyme was performed in two independent preparations of *Ucp2-WT* or *Ucp2-KO* BMDM. The values in nmol/min/mg protein after overnight exposure in EBSS were 3.4, 1.3 in *WT* and 4.2, 5.6 in *KO*. Similar values (5.1, 1.4 in *WT* and 5.8, 3.7 in *KO*) were obtained after overnight exposure in EBSS+Gln.

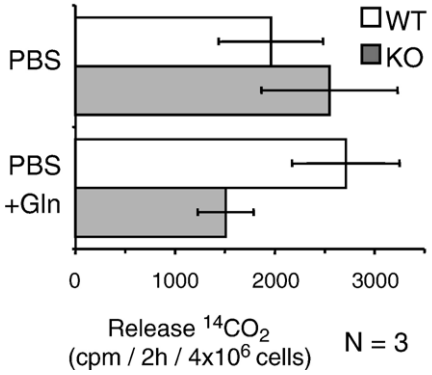


Fig. 7. Oxidation of radio labeled glutamine. Mean±s.e.m. of the carbon dioxide release from radio labeled glutamine obtained with BMDM that had been starved for 16 h in PBS "PBS" or BMDM that had been exposed for 16 h to PBS+Gln "PBS+Gln".

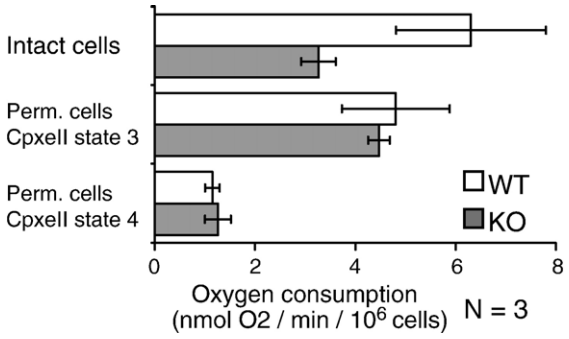


Fig. 8. Respiration of mitochondria in permeabilized BMDM. After the recording of cellular respiration of intact BMDM "Intact cells", the cells were permeabilized with digitonin (150 μM) in the presence of rotenone (1.25 μM) to allow recording of mitochondrial respiration in the presence of succinate (19 mM). This was made in the presence of ADP (1.5 mM): state 3 and then oligomycin (0.5 μg/ml) was added to record the state 4 rate. Values are shown as mean±s.e.m. of three independent experiments.

Therefore, no indication for a deficiency in the activity of enzymes of glutamine metabolism could be observed when *Ucp2-KO* BMDM was compared to *Ucp2-WT* BMDM.

The release of carbon dioxide from radio labeled glutamine was estimated (Fig. 7). When BMDM had not been exposed to glutamine the rate of oxidation is similar in the two types of cells whereas after exposure to glutamine the relative rates of *Ucp2-KO* and *Ucp2-WT* BMDM seemed to differ to an extent similar to that observed with cellular respiration or ammonium release (Fig. 5).

Permeabilization of BMDM by digitonin allowed to study BMDM mitochondria oxidizing succinate. In these experiments identical activity of mitochondria in *Ucp2-KO* BMDM and *Ucp2-WT* BMDM in phosphorylating state 3 and state 4 contrasted with the difference observed in intact cells (Fig. 8). Therefore, activities of complexes II to IV as well as the coupled state of mitochondria appeared identical in both types of BMDM.

ATP/ADP ratio was estimated in BMDM after overnight incubation in EBSS in the presence of glutamine. Uncoupling

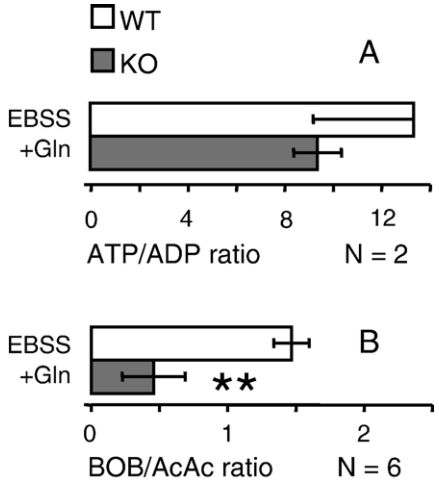


Fig. 9. ATP/ADP and BOB/AcAc concentration ratios. ATP/ADP ratio and beta-hydroxybutyrate (BOB)/acetoacetate (AcAc) ratio were determined in BMDM that had been incubated overnight in EBSS±2 mM glutamine. The number of independent experiments (*N*) is indicated, mean values are shown ±s.e.m. $^{**}P<0.01$ (*t* test).

was expected to decrease this ratio in *Ucp2-KO* BMDM. This was not the case (Fig. 9A). β-hydroxybutyrate to acetoacetate ratio was used as an index of intra-mitochondrial NADH/NAD ratio. It indicated a more reduced state of mitochondria in *Ucp2-WT* BMDM (Fig. 9B).

## 4. Discussion

Two characteristics of this study should be recalled: i) The BMDM used were in a non-activated state. Therefore, comparison with situations where activation of macrophages has taken place should be made with caution. ii) The important fuel glucose was kept to a physiological concentration of 5 mM. The relative differences between *Ucp2-KO* and *Ucp2-WT* BMDM were also found when BMDM had been incubated overnight in the presence of glutamine and in the absence of glucose *i.e.* PBS + glutamine (Fig. 5).

Entry of glutamine in the oxidative pathway involves glutaminase that releases ammonium and produces glutamate (step 1 in Fig. 1). Entry of glutamate into the Krebs cycle can occur through oxidative deamination by glutamate dehydrogenase (2a in Fig. 1) yielding a second ammonium ion or transamination (2b in Fig. 1), for which an obvious candidate is oxaloacetate yielding aspartate. In this scheme there are two glutamine end products that need to be eliminated somehow. One is ammonium, the other is aspartate. *Ucp2-WT* and *Ucp2-KO* BMDM clearly differed by their relative accumulation of these two metabolites (Figs. 3–6). At this point, it should be precised that measurements of intracellular content in amino acids or ammonium do not provide absolute values of the fluxes of metabolites but provided an estimation of the relative difference in the production rate of these molecules within the two types of BMDM.

After prolonged exposure to glutamine the respiratory rate of *Ucp2-WT* was higher than that of *Ucp2-KO* cells. Experiments with permeabilized BMDM (Fig. 8) showed that the functional state of mitochondrial complexes II–V is not different in both types of BMDM. This rules out the possibility that the decreased respiratory rate of *Ucp2-KO* BMDM would be due to a general decline of mitochondria in *Ucp2-KO* BMDM exposed to glutamine for several hours. Use of oligomycin, and estimation of ATP/ADP ratio in BMDM revealed unchanged coupling parameters. This was also the case when BMDM mitochondria were examined more directly (Fig. 8). This argues against uncoupling activity of UCP2 to be the explanation for the observed increase in respiratory rate and glutamine catabolism in *Ucp2-WT* BMDM. Actually, the increased reduced state of coenzymes observed in *Ucp2-WT* BMDM provides the alternate explanation that a more intense substrate supply to the mitochondrial respiratory chain would be the reason for the increase in respiratory rate in *Ucp2-WT* BMDM. In the absence of uncoupling activity (proton transport), another transport activity across the mitochondrial inner membrane is expected to explain the effect of UCP2 in BMDM. Obviously, UCP2 is not required for entry of glutamine into mitochondria since intra-mitochondrially produced metabolites accumulate (Figs. 1 and 3–6).

During the first hours of glutamine exposure apparition of metabolites was identical in both types of BMDM (Fig. 6). It was also observed that in PBS + Gln accumulation of aspartate was approximately four times more intense than in EBSS + Gln with identical relative difference between *KO* and *WT* (Fig. 5C). Therefore, it appears unlikely that a constitutive limitation in activity of either glutaminase or transaminase could be the explanation for increased accumulation of aspartate in *Ucp2-KO* BMDM.

The defect in *Ucp2-KO* BMDM appears as a delayed phenomenon resulting in failure to maintain or to induce an oxidative metabolism as intense as the *WT* does (Figs. 5A and 7). This delayed effect of UCP2 absence has to be considered in parallel with the fact that glutamine exposure of the cells stimulates translation of UCP2 mRNA and thus increases mitochondrial UCP2 content [19]. This stimulation takes approximately 2 h to reach its maximal intensity [19]. Establishment of differences between *Ucp2-KO* and *Ucp2-WT* BMDM (Fig. 6) appears therefore to correlate with the time needed to reach the maximal expression of UCP2.

In a recent study we propose that UCP2 would control the balance between oxidative metabolism (fatty acid oxidation) and glucose metabolism in mouse embryonic fibroblasts [26]. The availability of pyruvate to mitochondria was proposed as the target for UCP2 or UCP3 action [25,26]. In these studies emphasis was put on the relative importance of the strictly oxidative catabolism of fatty acids [26] or of galactose [25] with regard to the use of glucose. The mere observation of the relative production of metabolites in BMDM in the present study suggests that when glutamine is offered UCP2 promotes a complete oxidation with enhanced release of ammonium and conversely UCP2 absence results in an incomplete oxidation characterized by increased aspartate production, and limited supply of reduced coenzymes to the mitochondrial respiratory chain. It is likely that this role of UCP2 as a regulator of oxidative metabolism is not restricted to macrophages as glutamine exposure increases translation of UCP2 mRNA in all the different cell types examined so far [19].

Associated with data from other groups [27–29], our work reinforces the hypothesis that the physiological role of UCP2 is the control of how/which mitochondrial substrates are used (Fig. 1 "UCP2 B"). This effect of UCP2 occurred in the absence of stimulation of its uncoupling activity. Therefore, although the exact mechanism (transport activity of UCP2) remains to be determined, this report represents a landmark in understanding the importance of UCP2 for cellular metabolism.

## Acknowledgements

This work was supported by the Centre National de la Recherche Scientifique (CNRS), by ECFP6 funding in aid of the European Union (contract no. LSHM-CT-2003-503041), by the Ministère de la Recherche, and by the Institut National de la Santé et Recherche Médicale (INSERM). YE is supported by a grant from the Ministère de la Recherche and TN receives ECFP6 funding. We thank D. Chamereau for the help in the breeding of mice. We thank Dr. J. Bastin, Dr. F. Djouadi and Dr. J-L. Danan Dr. B. Bois-Joyeux and Dr. B. Miroux for their help during this study. We thank all staff-members of the Department of

Metabolism and Biochemistry (Service de Biochimie métabolique), Necker-Enfants Malades Hospital for technical assistance.

## References

[1] C. Fleury, M. Neverova, S. Collins, S. Raimbault, O. Champigny, C. Levi-Meyrueis, F. Bouillaud, M.F. Seldin, R.S. Surwit, D. Ricquier, C.H. Warden, Uncoupling protein-2: a novel gene linked to obesity and hyperinsulinemia, Nat. Genet. 15 (1997) 269–272.
[2] G. Mattiasson, P.G. Sullivan, The emerging functions of UCP2 in health, disease, and therapeutics, Antioxid. Redox Signal. 8 (2006) 1–38.
[3] S. Rousset, Y. Emre, O. Join-Lambert, C. Hurtaud, D. Ricquier, A.M. Cassard-Doulcier, The uncoupling protein 2 modulates the cytokine balance in innate immunity, Cytokine 35 (2006) 135–142.
[4] D. Ricquier, F. Bouillaud, The uncoupling protein homologues: UCP1, UCP2, UCP3, StUCP and AtUCP, Biochem. J. 345 (Pt 2) (2000) 161–179.
[5] J. Nedergaard, D. Ricquier, L.P. Kozak, Uncoupling proteins: current status and therapeutic prospects, EMBO Rep. 6 (2005) 917–921.
[6] V.P. Skulachev, Uncoupling: new approaches to an old problem of bioenergetics, Biochim. Biophys. Acta 1363 (1998) 100–124.
[7] J.F. Turrens, Superoxide production by the mitochondrial respiratory chain, Biosci. Rep. 17 (1997) 3–8.
[8] A. Negre-Salvayre, C. Hirtz, G. Carrera, R. Cazenave, M. Troly, R. Salvayre, L. Penicaud, L. Casteilla, A role for uncoupling protein-2 as a regulator of mitochondrial hydrogen peroxide generation, Faseb J. 11 (1997) 809–815.
[9] T. Nubel, D. Ricquier, Respiration under control of uncoupling proteins: clinical perspective, Horm. Res. 65 (2006) 300–310.
[10] D. Arsenijevic, H. Onuma, C. Pecqueur, S. Raimbault, B.S. Manning, B. Miroux, E. Couplan, M.C. Alves-Guerra, M. Goubern, R. Surwit, F. Bouillaud, D. Richard, S. Collins, D. Ricquier, Disruption of the uncoupling protein-2 gene in mice reveals a role in immunity and reactive oxygen species production, Nat. Genet. 26 (2000) 435–439.
[11] M.C. Alves-Guerra, S. Rousset, C. Pecqueur, Z. Mallat, J. Blanc, A. Tedgui, F. Bouillaud, A.M. Cassard-Doulcier, D. Ricquier, B. Miroux, Bone marrow transplantation reveals the in vivo expression of the mitochondrial uncoupling protein 2 in immune and nonimmune cells during inflammation, J. Biol. Chem. 278 (2003) 42307–42312.
[12] Y. Bai, H. Onuma, X. Bai, A.V. Medvedev, M. Misukonis, J.B. Weinberg, W. Cao, J. Robidoux, L.M. Floering, K.W. Daniel, S. Collins, Persistent nuclear factor-kappa B activation in Ucp2$^{-/-}$ mice leads to enhanced nitric oxide and inflammatory cytokine production, J. Biol. Chem. 280 (2005) 19062–19069.
[13] C.Y. Zhang, G. Baffy, P. Perret, S. Krauss, O. Peroni, D. Grujic, T. Hagen, A.J. Vidal-Puig, O. Boss, Y.B. Kim, X.X. Zheng, M.B. Wheeler, G.I. Shulman, C.B. Chan, B.B. Lowell, Uncoupling protein-2 negatively regulates insulin secretion and is a major link between obesity, beta cell dysfunction, and type 2 diabetes, Cell 105 (2001) 745–755.
[14] Y. Emre, C. Hurtaud, T. Nubel, F. Criscuolo, D. Ricquier, A.M. Cassard-Doulcier, Mitochondria contribute to LPS-induced MAPK activation via uncoupling protein UCP2 in macrophages, Biochem. J. 402 (2) (2007) 271–278.
[15] P. Newsholme, S. Gordon, E.A. Newsholme, Rates of utilization and fates of glucose, glutamine, pyruvate, fatty acids and ketone bodies by mouse macrophages, Biochem. J. 242 (1987) 631–636.
[16] T.C. Curi, M.P. De Melo, R.B. De Azevedo, T.M. Zorn, R. Curi, Glutamine utilization by rat neutrophils: presence of phosphate-dependent glutaminase, Am. J. Physiol. 273 (1997) C1124–1129.
[17] C. Pecqueur, M.C. Alves-Guerra, C. Gelly, C. Levi-Meyrueis, E. Couplan, S. Collins, D. Ricquier, F. Bouillaud, B. Miroux, Uncoupling protein 2, in vivo distribution, induction upon oxidative stress, and evidence for translational regulation, J. Biol. Chem. 276 (2001) 8705–8712.
[18] C. Hurtaud, C. Gelly, F. Bouillaud, C. Levi-Meyrueis, Translation control of UCP2 synthesis by the upstream open reading frame, Cell Mol. Life Sci. 63 (2006) 1780–1789.
[19] C. Hurtaud, C. Gelly, Z. Chen, C. Levi-Meyrueis, F. Bouillaud, Glutamine stimulates translation of uncoupling protein 2mRNA, Cell Mol. Life Sci. 64 (14) (2007) 1853–1860.
[20] F. Criscuolo, J. Mozo, C. Hurtaud, T. Nubel, F. Bouillaud, UCP2, UCP3, avUCP, what do they do when proton transport is not stimulated? Possible relevance to pyruvate and glutamine metabolism, Biochim. Biophys. Acta 1757 (2006) 1284–1291.
[21] J. Xaus, M. Comalada, A.F. Valledor, J. Lloberas, F. Lopez-Soriano, J.M. Argiles, C. Bogdan, A. Celada, LPS induces apoptosis in macrophages mostly through the autocrine production of TNF-alpha, Blood 95 (2000) 3823–3831.
[22] D. Haussinger, W. Gerok, H. Sies, Inhibition of pyruvate dehydrogenase during the metabolism of glutamine and proline in hemoglobin-free perfused rat liver, Eur. J. Biochem. 126 (1982) 69–76.
[23] T. Bücher, in: H. Sund (Ed.), Pyridine Nucleotides Dependent Dehydrogenases, Springer-Verlag, New York, 1970, p. 439–461.
[24] A. Vassault, J. Bonnefont, N. Specola, J. Saudubray. in: Hommes, F., (Ed.), Techniques in Diagnosic Human Biochemical Genetics: a Laboratory Manual, Wiley-Liss, A John Wiley and Sons, INC, New York 1991, pp. 285–308.
[25] J. Mozo, G. Ferry, A. Studeny, C. Pecqueur, M. Rodriguez, J.A. Boutin, F. Bouillaud, Expression of UCP3 in CHO cells does not cause uncoupling, but controls mitochondrial activity in the presence of glucose, Biochem. J. 393 (2006) 431–439.
[26] C. Pecqueur, T. Bui, C. Gelly, J. Hauchard, C. Barbot, F. Bouillaud, D. Ricquier, B. Miroux, C.B. Thompson, Uncoupling protein-2 controls proliferation by promoting fatty acid oxidation and limiting glycolysis-derived pyruvate utilization, Faseb J. (in press) (Electronic publication ahead of print).
[27] L. Millet, H. Vidal, F. Andreelli, D. Larrouy, J.P. Riou, D. Ricquier, M. Laville, D. Langin, Increased uncoupling protein-2 and -3 mRNA expression during fasting in obese and lean humans, J. Clin. Invest. 100 (1997) 2665–2670.
[28] P. Schrauwen, G. Schaart, W.H. Saris, L.J. Slieker, J.F. Glatz, H. Vidal, E.E. Blaak, The effect of weight reduction on skeletal muscle UCP2 and UCP3 mRNA expression and UCP3 protein content in Type II diabetic subjects, Diabetologia 43 (2000) 1408–1416.
[29] J. Himms-Hagen, M.E. Harper, Physiological role of UCP3 may be export of fatty acids from mitochondria when fatty acid oxidation predominates: a hypothesis, Exp. Biol. Med. (Maywood) 226 (2001) 78–84.